



Stereo bathymetry to monitor small seasonal agriculture water ponds in ungauged areas

Victoria Vanthof, Sylvain Ferrant, Romain Walcker, Richard Kelly

► To cite this version:

Victoria Vanthof, Sylvain Ferrant, Romain Walcker, Richard Kelly. Stereo bathymetry to monitor small seasonal agriculture water ponds in ungauged areas. ISPRS International Archives of the Photogrammetry, Remote Sensing and Spatial Information Sciences, 2024, 48 (3), pp.565 - 570. <10.5194/isprs-archives-xxviii-3-2024-565-2024>. <hal-04778781>

HAL Id: hal-04778781

<https://hal.science/hal-04778781v1>

Submitted on 12 Nov 2024

HAL is a multi-disciplinary open access archive for the deposit and dissemination of scientific research documents, whether they are published or not. The documents may come from teaching and research institutions in France or abroad, or from public or private research centers.

L'archive ouverte pluridisciplinaire **HAL**, est destinée au dépôt et à la diffusion de documents scientifiques de niveau recherche, publiés ou non, émanant des établissements d'enseignement et de recherche français ou étrangers, des laboratoires publics ou privés.



Distributed under a Creative Commons CC BY 4.0 - Attribution - International License

Stereo bathymetry to monitor small seasonal agriculture water ponds in ungauged areas

Victoria Vanthof¹, Sylvain Ferrant², Romain Walcker³, Richard Kelly⁴

¹ Dept. of Environment, University of Waterloo, Waterloo, Ontario, Canada - vrvantho@uwaterloo.ca

² CESBIO, Université de Toulouse 3, CNES/CNRS/INRAE/IRD/UT3, 31401 Toulouse, France - sylvain.ferrant@ird.fr

³ CRBE, Université de Toulouse 3, CNRS, IRD, INPT, 31401 Toulouse, France - romain.walcker@univ-tlse3.fr

⁴ Dept. of Environment, University of Waterloo, Waterloo, Ontario, Canada - rejkelly@uwaterloo.ca

Keywords: tank hydrology, bathymetry, Pléiades stereoscopy, volume uncertainty

Abstract

Small reservoirs represent a critical water supply to farmers across semi-arid regions, but their hydrological modelling suffers from data scarcity and highly variable and localised rainfall intensities. Over 200,000 ancient rainwater harvesting reservoirs ("tanks") exist across South India, but with their complex history, considerable size variation, and widespread distribution, understanding the hydrological role of these tanks has been difficult. Fortunately, the last decade has seen improvements in sensors and technologies that enhance our ability to assess the hydrological role of these tanks. In particular, high-resolution Digital Elevation Model (DEMs), now much easier to produce, can be used to improve the characterization of tanks and their surrounding watersheds. Here, a high-resolution DEM is created during the lowest reservoir conditions using Pléiades stereoscopy, and along with two global DEMs, compared with volume estimates from a field-derived UAV reference DEM for a set of tanks in South India. This study demonstrates that a Pléiades-derived DEM can capture accurate reservoir geometry and, when simulating water volume, achieves volumetric differences of 2-8% compared to our UAV reference data. The Pléiades-derived-DEM produced an equivalent height bias less than the expected bias for the recently launched Surface Water and Ocean Topography (SWOT) mission. Deriving high-resolution tank bathymetry from space during low-water conditions provides an opportunity to systematically and repeatably measure tank volume. These results are encouraging in efforts to utilize very high resolution DEMs chosen at an appropriate hydrological time, particularly in regions where water management and security is paramount.

1. Introduction

Water security is a critical concern in regions affected by climate change, especially in semi-arid agricultural systems. Across India are thousands of millennia-old small rainwater harvesting reservoirs ("tanks"). These reservoirs are often disconnected from perennial rivers, fed entirely by monsoon rainfall, and were once solely used for small-holder irrigation. Changing cropping patterns, climate change, and the overconsumption of groundwater are renewing interest in tanks to sustain irrigation and enhance aquifer recharge (Glendenning et al., 2012). While increasing the number of functioning tanks in upstream regions is a common adaptation to water stressors, this approach is unknown to benefit water security across South India. Understanding the role of tanks on regional hydrology has been limited because of sparse and infrequent data. Over 200,000 tanks exist in South India alone which impedes the use of only field-based sampling approaches (Gunnell and Krishnamurthy, 2003). Fortunately, improvements in satellite remote sensing brings new opportunities to observe tanks across South India from space.

Quantifying tank storage capacity and monitoring their seasonal fluctuations is critical to understanding their regional hydrology over larger spatial scales (Bitterman et al., 2016). With frequent tank volume estimates, tank state can be modelled more accurately—with either a strictly remote sensing monitoring approach, or basin-scale physical models, or a combination of these. Tank volume in this region is often neglected or approximated in previous basin-scale physical hydrological modeling studies because input parameters are lacking. Lacking these, remote sensing is a critical tool to overcome the difficulty of accessing reliable information on tank storage (Vanthof and Kelly,

2019). If more field-based observations are ultimately collectible, remote sensing and modeling efforts will only improve.

Tank storage across the Indian Rainwater Harvesting System (RHS) is challenging to retrieve from current remote sensing techniques and observations because of their small size, ephemeral filling behavior, and scattered (but dense) network on the landscape. The general procedure for space-based reservoir storage estimation associates water surface elevation and area. Although there is no universal definition for small reservoirs, here small reservoir is defined to have a water surface extent less than 50 ha in size. Water extent can be retrieved from several different multispectral and radar sensors. However, to convert water extent to storage estimates, water height is needed. Satellite radar and laser altimetry are the predominant approaches for estimating water height in small reservoirs. These techniques, however, do not provide sufficient spatial or temporal resolution for the scattered hydrological network of the RHS. Most tanks do not intersect current altimetry tracks (ie, ICESat 2, Sentinel-3) or fill and empty faster than satellite re-visits. This was shown recently for a dense network of West African lakes where Sentinel-3 altimeter tracks only covered 1% of the regional lakes (de Fleury et al., 2023). A second approach to retrieve water height is to capture reservoir bathymetry or topography. Satellite water areas can be paired directly within the bathymetry to estimate storage. A common approach when bathymetry is not available for all reservoirs is to assume that, in similar geological situations, their shapes are not very different. This allows rating curves to be developed and volume to be estimated with satellite water area alone (Vanthof and Kelly, 2019). However, the suitability of generalized equations will depend on the region, the complexity of reservoir shape and sizes, and the quality of the Digital Elevation Model (DEM)

used to extract the topography.

Despite advancements in global elevation products for tank bathymetry, their small size impedes systematic capacity retrieval. Current global DEM products have shown some promise for tank bathymetry retrieval but often did not capture tank topography (Vanthof and Kelly, 2019). While the 12-m TanDEM-X DEM product showed promise in Vanthof and Kelly (2019) its utility was limited by vegetation and water presence during acquisition. Utilizing very high-resolution (VHR) stereoscopic images during dry conditions offers an opportunity for detailed tank topography retrieval, as demonstrated by Pascal et al. (2021). However, the accuracy of volumetric estimation using a stereoscopic-derived DEM remains uncertain and requires testing in the context of tanks across India. Here a 2m derived DEM from Pléiades stereoscopy is compared to field-observed bathymetry for a set of tanks without water to evaluate its use for tank bathymetry retrieval and volume estimation. Two additional global DEMs are included to evaluate how existing DEMs compare.

2. Materials and Methods

2.1 Study Area

The Gundar River Basin, located in Tamil Nadu, India, contains over 2,000 tanks and receives an average annual rainfall of 770 mm, with the Northeast (NE) monsoon contributing 50% of the rainfall from October to December (Figure 2). Tanks fill seasonally and are typically dry outside the monsoon seasons, allowing their topography to be observed remotely without water. This study focuses on a small area in the middle of the basin, chosen for its accessible tanks and support from the DHAN Foundation, a local NGO, for data collection. The area contains 150 tanks of varying shapes and sizes, four of which are used as the field site for this study (Figure 1).

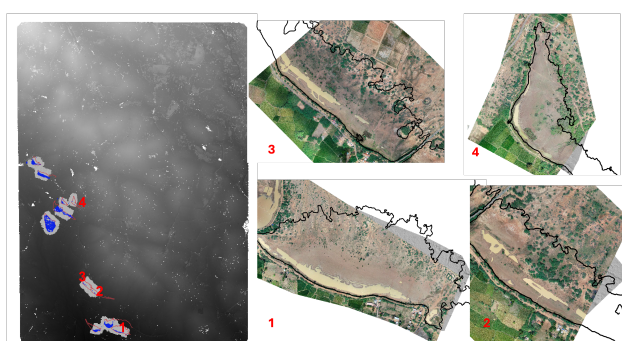


Figure 1. Examples of four surveyed field tanks. Tank 1 contains minimal vegetation and tank 2-3 contain the most. Pleiades © CNES 2023 Distribution Airbus DS.

Tanks are connected in a cascading fashion with two structural elements, which include a waterspread area and a command area. First, water is impounded behind an earthen crescent shaped embankment, known as a bund. Water pools upstream of the bund and forms the water spread area. The water is subsequently released through manual sluices into canals that distribute the water to irrigated lands, known as the command area. Across the region tanks exist in various states of operation: some are well maintained and operating efficiently, others are unmaintained and operate in a limited way or not

at all. Unmaintained tanks often have encroachment of mesquite vegetation into the tank waterspread area (Figure 1) and/or abandonment of the command area. These conditions cause a fragmented landscape of hydrologically disconnected tanks.

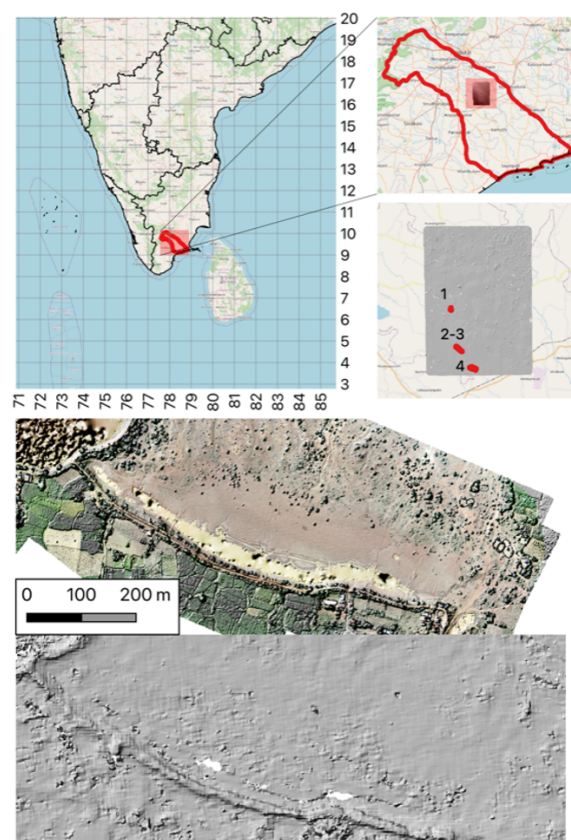


Figure 2. Study Area map showing 4 tank locations for UAV survey. Bottom shows UAV DEM for tank 4 (top) and Pléiades DEM for tank 4 (bottom). Pleiades © CNES 2023 Distribution Airbus DS.

2.2 UAV Field Validation

A UAV field survey was conducted on December 31, 2022, over these four tanks to create a VHR DEM to be used as a reference dataset (Figure 2). An example of the UAV-derived DEM is shown in Figure 2. These tanks were selected because they had low water (less than 2%) in the waterspread area and different levels of vegetation presence (Figure 1).

2.3 UAV-SfM DEM

The survey utilized a DJI Phantom 4 UAV equipped with standard RGB lenses, flying at an altitude of 120 m and a speed of 12 m/s. To ensure positional accuracy during post-processing, twenty-seven ground control points (GCPs) were established across the site using Real-Time Kinematic (RTK) and a base station for precise geometric and orthometric rectification. The UAV data was processed by stitching observations together using Structure from Motion (SfM) techniques with Agisoft software and was corrected based on the GCP measurements.

To assess satellite-derived tank bathymetry, it is important that our UAV-SfM DEM (our primary validation) accurately represents the tank bathymetry. The initial DEM elevation values

do not represent the ground in cases where there is mesquite vegetation or if water was in the waterspread area during the flight (Figure 1). To create a bare-earth validation DEM three main steps were followed. First, water pixels were masked in the UAV-SfM DEM for each tank and filled the missing elevation pixels using an inverse distance weighting (IDW) approach. To isolate vegetation in the DEM, a slope-based Digital Surface Model (DSM) filter was applied to the tank waterspread area and the bund separately. Separating the bund and the waterspread area was important because a single value either smoothed the bund, which caused inaccurate geometry, or missed small patches of trees in the waterspread area. For the waterspread area a slope filter of 5 degrees was applied to isolate trees, and for the bund, a slope filter of 30 degrees was used. The identified vegetation pixels were then removed from the original UAV-SfM DEM and the missing pixels filled with IDW elevation values. This resulted in a vegetation-free UAV-SfM DEM for four tanks (Figure 3).

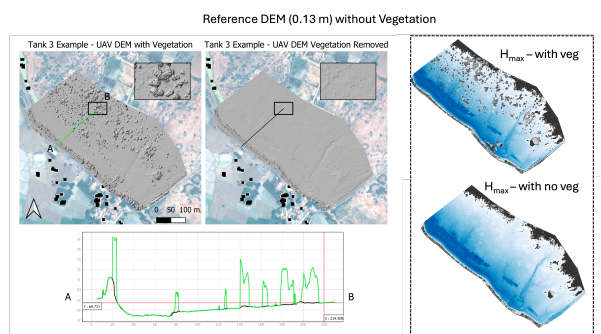


Figure 3. Example of vegetation removed from UAV DEM for tank 3. Green line in profile is UAV with vegetation and the black line is vegetation removed. The filled water for tank 3 provide an example of what hmax would look like with and without vegetation. Pléiades © CNES 2023 Distribution Airbus DS.

2.4 Spaced-based DEMs

Several DEMs with a range of horizontal resolutions were used to estimate tank volumes and compared with the four field surveyed tanks. All DEMs were transformed to WGS84 using a nearest-neighbor resampling, and for any DEMs not initially using EGM96, vertical datum shifts were applied using the 'demgeoid' function in the NASA Ames Stereo-Pipeline (ASP) toolbox.

2.4.1 Pléiades DEM: The Pléiades stereoscopic images used in this study include one stereo-pair acquired in May 2023 (specifically tasked for the purpose of this study). The images were acquired in the dry-season when tanks are empty. A 2m resolution DEM was generated using the panchromatic stereoscopic images and the NASA ASP software. The photogrammetric process was done using the rational polynomial coefficient provided by the satellite operator. A point cloud was first generated from the panchromatic images with the block matching algorithm of the stereo utility in ASP. Second, the point cloud was rasterized on a 2m resolution UTM grid using the point2dem tool in ASP. Using the reflectance data a Normalized Difference Vegetation Index (NDWI) index was calculated and a threshold applied to create a water mask. Pixels that corresponded to water in the mask were set as No-Data values in

the DEM. While the Pléiades DEM is a DSM, early comparisons of the UAV DEM and the Pléiades DEM, revealed that most small patches of vegetation were smoothed out in the Pléiades DEM. However, larger patches of vegetation were present and removed from the waterspread area with a slope filter of 10 degrees. This also removed erroneous noise pixels that lead to troughs of several meters in the tank bed.

2.4.2 TanDEM-X DEM: The TanDEM-X DEM at 12m was acquired through a scientific call from the German Aerospace Centre (DLR). DLR produced the DEM from a five year (2010–2015) TanDEM-X mission using InSAR methods. The good performance of the DEM has been reported, with a final global absolute vertical accuracy of 3.49m and relative vertical accuracy of 0.99 and 1.37m on flat and steep terrain, respectively (Rizzoli et al., 2017). These results are in line with Vanthof and Kelly (2019) who reported a vertical absolute accuracy ranging from 0.98-1.47 m.

2.4.3 Copernicus DEM: The 30m resolution global Copernicus DEM (GLO-30) was released in 2021 by the European Space Agency (ESA) and AIRBUS. It is based on the WorldDEM, which is in turn based on edited and smoothed radar satellite data acquired during the TanDEM-X mission. The relative vertical accuracy is smaller than 2m for flat slopes and less than 4m on steep slopes (Purinton and Bookhagen, 2021). Although this DEM is coarser than the TanDEM-X DEM it is expected to have fewer anomalies because it has been edited to a DSM. Purinton and Bookhagen (2021) found that the GLO-30 is the highest-quality landscape representation and should be the preferred DEM for topographic analysis in areas that lack higher-resolution DEMs.

2.5 Reservoir Inventory and Maximum Height Definition

With each DEM, a possible maximum water extent when the tank is in a filled state needs to be defined. To do this, the maximal water area extent (MWAE) is defined using PlanetFusion multispectral observations. PlanetFusion is an Analysis Ready dataset produced by PlanetLabs providing daily 3m resolution images by combining PlanetScope scenes and calibrated with publicly available multispectral satellites (i.e., Sentinel-2, Landsat, MODIS, and VIIRS) (Houborg and McCabe, 2018). Sentinel-2 observations likely would also provide sufficient spatial resolution, however the temporal resolution of PlanetFusion offers a better chance of assessing water presence during cloudy periods. PlanetFusion observations (R, G, B, NIR) from 2018-2022 were filtered to correspond to the NE monsoon season, and an NDWI band was added to each image. The maximum NDWI pixel value was retrieved to create a raster image corresponding to the wettest pixel over the four-year period. The PlanetFusion MWAE was then created by applying a threshold of -0.1 to segment water from land. The PlanetFusion MWAE was converted to polygons and filtered by removing (i) tanks containing more than 5% of Pléiades 2m DEM no-data and (ii) water extents less than 1,000 m², which are considered small temporary ponds and not tanks. The PlanetFusion MWAE was after intersected with elevation contours derived from the Pléiades VHR DEM to select a closed isoline that matched most closely with the PlanetFusion MWAE. This isoline — defined with visual inspection — corresponds to a water height surrounding the surface water (i.e., the maximum elevation from the bottom of the depression). Only four of the 150 identified tanks identified above are the focus in this study.

2.6 Reservoir Volume Estimates

Across the 4 sensor approaches (UAV validation, Pléiades, TanDEM-X, GLO-30), a common methodology was used to estimate reservoir volume, similar to that described in Vanthof and Kelly (2019). For each of the four DEMs, the maximum height (h_{max}) is defined for each tank by intersecting the tank isoline defined above with each DEM. The median elevation value at the isoline is set for each DEM and used as h_{max} . Each DEM provided paired volume and area estimates at 5 cm height increments from the base of the tank to h_{max} . Here h_{max} is set based on contours and not as a standard bund height.

Hypsometric profiles were developed for all the four tanks from all DEMs. Since the height of the tank bottom is not known for each DEM, the reference is set to the reference DEM and all other methods are truncated to the minimum in-situ area and corresponding volume. This step ensures that all DEMs are standardized to the same base. Height-area and area-volume curves are interpolated to obtain height and volume matches with other DEMs.

2.7 Uncertainty Assessment

To evaluate the DEMs for the purpose of bathymetry retrieval, the DEMs were compared with the reference DEM at 0.13 m. Although the performance of a DEM is often assessed by considering its absolute vertical accuracy compared to a reference dataset, this approach does not inform on volumetric errors and is less informative when interested in relative pixel-to-pixel errors. Instead of absolute vertical accuracy we report i) the volume differences at different fill increments when compared to the reference DEM and ii) illustrate the differences in tank geometry.

3. Results

3.1 Representation of Tank Geometry

Figure 4 provides a visual 3-d profile representation for Tank 1 for all DEMs and a horizontal profile crossing the bund (label A on Figure 4) and waterspread area (label B). The Pléiades geometry of the tank closely matches the reference UAV surface across the waterspread area and the bund. This was the case for all four tanks. As shown by the transect profile, DEMs from TanDEM-X and GLO-30 fail to resolve the bund; in certain areas the GLO-30 DEM can misrepresent the bund entirely. More noise is evident in the TanDEM-X elevation values, which is not surprising as this product is a DSM with signal from vegetation and potentially water presence.

3.2 Hypsometric Profile

Figure 5 shows the volume-area curves by tank for each DEM. With the exception of Tank 1, the GLO-30 and Tandem-X DEM for the other three tanks were unable to produce accurate volume-area values for matching UAV areas. For example, when looking at tank 3 in Figure 5 for areas greater than 5000 m², the area no longer changed, which highlighted that the maximum extent of water was reached using the GLO-30. For all tanks, field-observed curves match closest with Pléiades DEM. The volume differences between Pléiades DEM and the UAV DEM vary as area increases and are not consistent between tanks. Although vegetation was removed in the waterspread area for the Pléiades and UAV DEMs, not all vegetation

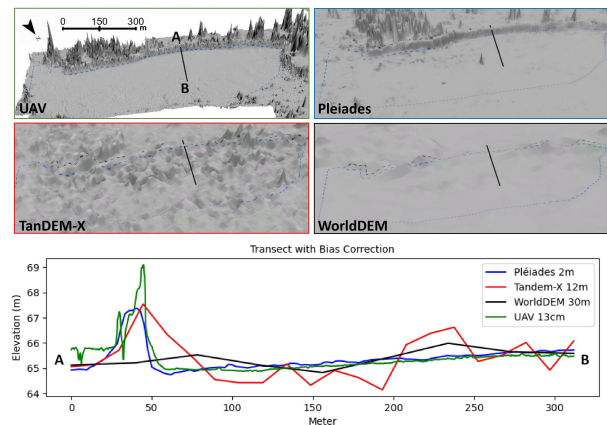


Figure 4. Visual 3-d profile representation for Tank 1 for all DEMs and a horizontal profile crossing the bund. Label A is the start of the bund and label B is within the waterspread area. Pléiades © CNES 2023 Distribution Airbus DS.

could be removed from the bund of the tank without modifying its geometry. As water area increases a larger portion of the bund will be included in the volume estimate and therefore vegetation on the bund could be impacting the larger volume differences. It should be noted that these tanks are different sizes and tank 1 is almost twice as large as the other three.

The Pléiades 2 m DEM height closely matches the UAV height at equivalent volume. Table 1 shows the equivalent height at maximum volume for each tank. This shows that at maximum water surface area, the Pléiades 2 m DEM height ranges from 1.23-7.95 cm for the four tank sample.

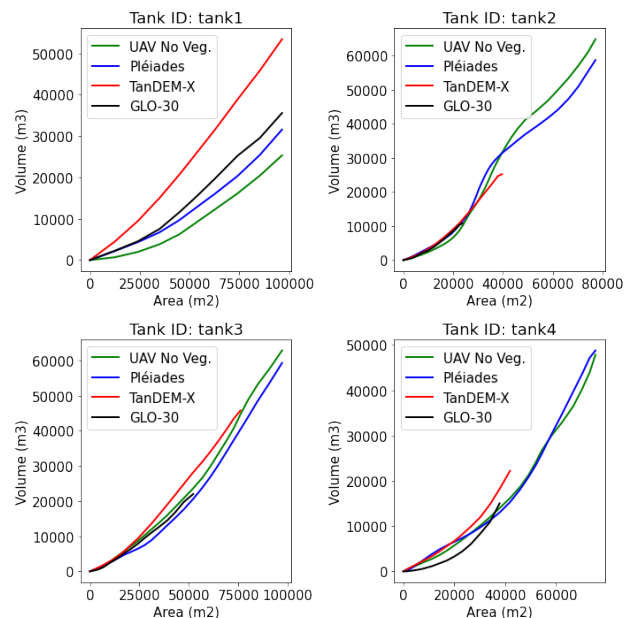


Figure 5. Volume-area curves for the four tanks. The reference is the UAV data in green compared to the GLO-30 DEM (black), TanDEM-X DEM (red) and the Pléiades DEM (blue).

3.3 Volume uncertainty assessment

Figure 6 shows the error as a percentage for each DEM at different fill levels. The fill level was calculated from the reference

Tank #	Area (m ²)	Volume Difference (m ³)	Equivalent Height (cm)
Tank 1	96375	6237	6.47
Tank 2	77122	6131	7.95
Tank 3	97021	3575	3.69
Tank 4	75537	933	1.23

Table 1. The volume difference and equivalent height between Pléiades and UAV at the same maximum water surface area.

Equivalent height is calculated as (Pléiades Volume - UAV Volume) / Area.

UAV volumes for each tank to provide a standardized metric to compare across all tanks. The error plot summarizes all percent error difference from Figure 5 to provide a better understanding of the volumetric differences between each DEM and our reference UAV DEM. At the lower fill volume (10-30%) all DEMs show minimal differences to the reference volumes. For the Tandem-X and the GLO-30, an increasing trend is shown between error and fill. The Pléiades volumes do not show an increases trend in error.

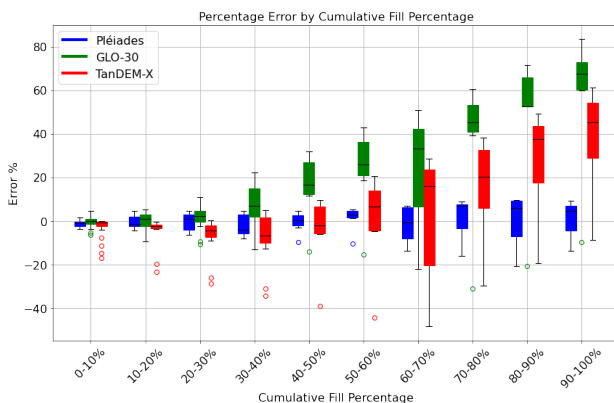


Figure 6. Percent error by standardized fill percentage for each tank.

Sensor	MAPE		
	Min	Max	Std Dev
Pléiades	1.94	7.64	3.18
GLO-30	11.14	23.17	18.68
TanDEM-X DEM	5.29	23.50	13.50

Table 2. MAPE Range and Average Standard Deviation by DEM in Volume (m³).

4. Discussion

4.1 Assessing small reservoir dynamics

In a comparison of three space-based bathymetries against UAV validation data, Pléiades performed well and far surpassed the quality of the other DEMs. Importantly, the Pléiades-derived DEM for the subset of tanks produced an equivalent height bias less than the expected bias for the recently launched Surface Water and Ocean Topography (SWOT) mission. The SWOT satellite is designed to achieve a vertical accuracy within 10 cm for reservoirs larger than 1 km² and within 25 cm for reservoirs larger than 0.0625 km². The tanks analyzed in this study have maximum fill levels ranging from 0.08 to 0.10 km². Our results demonstrated that a VHR DEM created from Pléiades data can capture volumes in small reservoirs with a vertical accuracy between 1.23 cm and 7.95 cm. This indicates that VHR DEMs, created during dry conditions, can complement SWOT measurements, particularly for reservoirs smaller than 1 km²,

where they can achieve greater precision than SWOT. The increasing availability of in-track stereo or multi-view stereo observations from VHR passive optical sensors, such as Pléiades, WorldView, and SkySat, holds significant potential for improving water management on a large scale. While global, lower-resolution space-based DEMs like TanDEM-X and GLO-30 remain useful, they lack the level of detail needed for accurate and widespread monitoring of tank volumes.

4.2 Limitations

Hundred of thousands of tanks exist across South India and in this work only a sample of four tanks were surveyed in the field. This sample helps to understand the use of different DEMs for tank volume estimation but given the large spread in volume error observed in Figure 6 for the TanDEM-X DEM and the GLO-30 DEM, these products should be used with caution when capturing volume at the tank level. The Pléiades DEM percent errors across all fills remain low, which shows promise for using the DEM more widely across tanks. Tanks with excessive vegetation, however, need to be screened and vegetation removed to retrieve tank topography. The impact of vegetation in our tank sample was minimal; however, mesquite vegetation can completely occupy the tank waterspread areas in some tanks in the basin.

To estimate tank volume the methodology relied on satellite bathymetry and used our reference dataset to assess volume differences. The UAV-SfM DEM was used as the ground-truth reference. However, like other DEMs, it is constructed from an airborne perspective, where overhanging trees or other vertical obstructions can hide features from observation point. While it was assumed errors are minimal for our reference DEM, they do still exist. Given the VHR of the reference DEM, shallow surface features are also captured that are unable to be captured with Pléiades because its 2m resolution has a smoothing effect. Although the reference DEM was captured during low-water conditions, water still had to be masked from the tank. This adds additional uncertainty as the base of the reference DEM is not set to its true elevation. While vegetation in the UAV-SfM DEM was removed from the tank waterspread area quite successfully, vegetation along the bund was more challenging to remove because it was on a slope. Although the other DEMs also contain vegetation, the impact of vegetation on the final elevation will be smaller due to their coarser resolution.

4.3 Next Steps

In recent years the TanDEM-X DEM has been used and applied for power type expressions for volume estimation in small storage structures (Karran et al., 2017, Rodrigues and Liebe, 2013, Vanthof and Kelly, 2019). Our results highlight how a 2 m Pléiades-derived DEM outperforms the TanDEM-X DEM for retrieving tank bathymetry. When applying power type expressions for volume estimation from bathymetric data, the error comes from three terms - DEM error, error from the power approximation, and error from satellite water extent. Here only the error from the DEM itself is presented. Future work will explore power type expressions for volume estimation across a larger set of tanks using the Pléiades DEM and attempt to separate these error terms as done by others (Brosens et al., 2022). The benefit of VHR DEMs chosen at an appropriate hydrological time, as done here for Pléiades stereoscopic images, is that they can be targeted when reservoir conditions are low (Pascal, 2021). Global DEMs do not offer this and are

static, which means that changing landscape conditions will inherently bring error. In the near future CO3D mission or the proposed Sentinel-HR missions could produce such on-demand VHR DEMs.

5. Conclusion

Deriving VHR tank bathymetry from space during low-water conditions provides an opportunity to systematically and repeatably measure tank volume. Previous global scale DEMs are too coarse for precise capacity estimates and over 200,000 tanks in South India impede the wide-spread use of UAV or Lidar approaches. Using a DEM derived from UAV field survey when tanks were empty, this study illustrated that a DEM at 2m from Pléiades stereoscopy can be used to accurately determine and predict the tank geometry during dry conditions. While the results of this study are site specific, tanks in the region share similar bund heights and sizes, highlighting that the Pléiades DEM will be highly accurate for them also. These results shall encourage hydrologists to use VHR DEMs chosen at an appropriate hydrological time - here an annual drought that characterize this south-Indian region.

Acknowledgements

The authors acknowledge the support from DLR (Germany) for access to TanDEM-X DEM data under the successful proposal DEMHYDR0751. We also thank the Development of Humane Action (DHAN) Foundation for generously sharing their experiences and helping facilitate field data collection. The Pleiades images acquisition was supported by the CNES through the DINAMIS program. Those images are commercial data that can be obtained via the website (<https://www.intelligenceairbusds.com/geostore/>).

References

- Bitterman, P., Tate, E., Van Meter, K. J., Basu, N. B., 2016. Water security and rainwater harvesting: A conceptual framework and candidate indicators. *Applied Geography*, 76, 75–84.
- Brosens, L., Campforts, B., Govers, G., Aldana-Jague, E., Razanamahandry, V. F., Razafimbelo, T., Rafolisy, T., Jacobs, L., 2022. Comparative analysis of the Copernicus, TanDEM-X, and UAV-SfM digital elevation models to estimate lavaka (gully) volumes and mobilization rates in the Lake Alaotra region (Madagascar). *Earth Surface Dynamics*, 10(2), 209–227. <https://esurf.copernicus.org/articles/10/209/2022/>.
- de Fleury, M., Kergoat, L., Grippa, M., 2023. Hydrological regime of Sahelian small waterbodies from combined Sentinel-2 MSI and Sentinel-3 Synthetic Aperture Radar Altimeter data. *Hydrology and Earth System Sciences*, 27(11), 2189–2204. <https://hess.copernicus.org/articles/27/2189/2023/>.
- Glendenning, C., van Ogtrop, F., Mishra, A., Vervoort, R., 2012. Balancing watershed and local scale impacts of rain water harvesting in India—A review. *Agricultural Water Management*, 107, 1–13.
- Gunnell, Y., Krishnamurthy, A., 2003. Past and Present Status of Runoff Harvesting Systems in Dryland Peninsular India: A Critical Review. *Ambio*, 32, 320–324.
- Houborg, R., McCabe, M. F., 2018. A Cubesat enabled Spatio-Temporal Enhancement Method (CESTEM) utilizing Planet, Landsat and MODIS data. *Remote Sensing of Environment*, 209, 211–226.
- Karran, D. J., Westbrook, C. J., Wheaton, J. M., Johnston, C. A., Bedard-haughn, A., 2017. Rapid surface-water volume estimations in beaver ponds. *Hydrology and Earth System Sciences*, 21, 1039–1050.
- Pascal, C. Sylvain Ferrant, A. S. J.-C. M. S. G. e. a., 2021. HighResolution Mapping of Rainwater Harvesting System Capacity from Satellite Derived Products in South India. *2021 IEEE International Geoscience and Remote Sensing Symposium*, 7011–7014.
- Purinton, B., Bookhagen, B., 2021. Beyond Vertical Point Accuracy: Assessing Inter-pixel Consistency in 30 m Global DEMs for the Arid Central Andes. *Frontiers in Earth Science*, 9.
- Rizzoli, P., Martone, M., Gonzalez, C., Wecklich, C., Borla Tridon, D., Bräutigam, B., Bachmann, M., Schulze, D., Fritz, T., Huber, M., Wessel, B., Krieger, G., Zink, M., Moreira, A., 2017. Generation and performance assessment of the global TanDEM-X digital elevation model. *ISPRS Journal of Photogrammetry and Remote Sensing*, 132, 119–139.
- Rodrigues, L. N., Liebe, J., 2013. Small reservoirs depth-area-volume relationships in Savannah Regions of Brazil and Ghana. *Water Resources and Irrigation Management*, 2, 1–10.
- Vanthof, V., Kelly, R., 2019. Water storage estimation in ungauged small reservoirs with the TanDEM-X DEM and multi-source satellite observations. *Remote Sensing of Environment*, 235, 111437.